

Supporting Information

Photochemical coupling reactions between Fe(III)/Fe(II), Cr(VI)/Cr(III) and polycarboxylates: inhibitory effect of Cr species

*Zhaohui Wang, Wanhong Ma, Chuncheng Chen, and Jincai Zhao**

Beijing National Laboratory for Molecular Sciences, Key Laboratory of Photochemistry, Institute of
Chemistry, The Chinese Academy of Sciences, Beijing 100190, China

14 pages

10 figures

2 tables

1 scheme

* Corresponding author fax: +86-10-8261-6495; e-mail: jczhao@iccas.ac.cn.

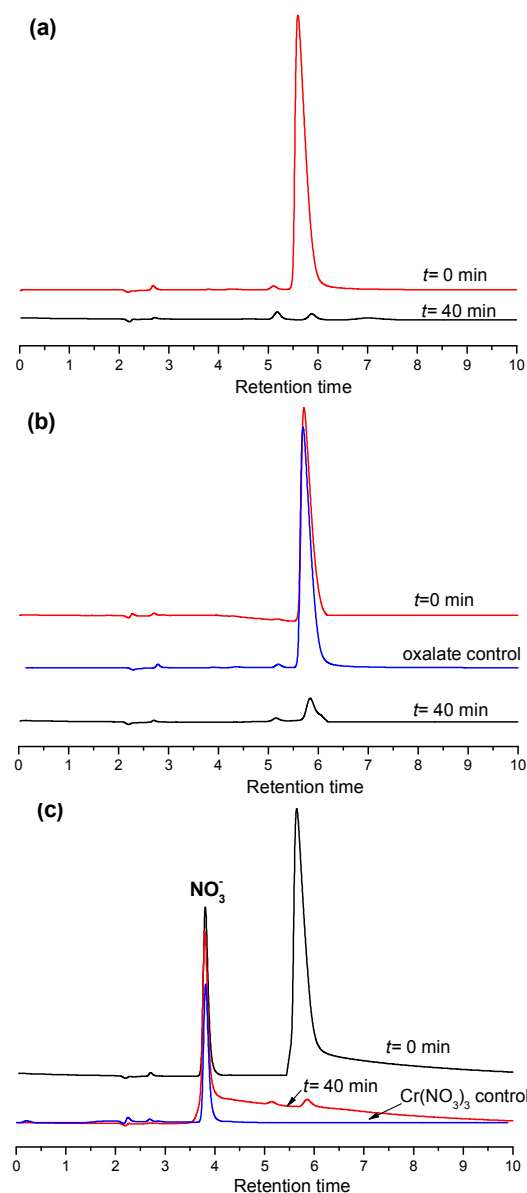


Figure S1. Ion chromatograph spectra of oxalate measured before and after photochemical reaction. (a) Fe(III)/ox; (b) Fe(III)/ox/Cr(VI); (c) Fe(III)/ox/Cr(III). Fe(III), 100 μM ; oxalic acid, 500 μM ; Cr(VI) or Cr(III), 80 μM , pH 3.0. 500 μM oxalate and 80 μM $\text{Cr}(\text{NO}_3)_3$ as control in (a) and (c). 10 mM NaOH as eluent.

As observed in Figure S4, after 40 min of irradiation, the TOC values became constant whereas definite amounts of oxalate were detected in alkaline media by ion chromatograph (IC) (Figure S1a). Based on this result, we conclude that these kinds of Cr-oxalate complexes are liable to decompose in alkaline media and therefore release oxalate, which was easily measured by IC.

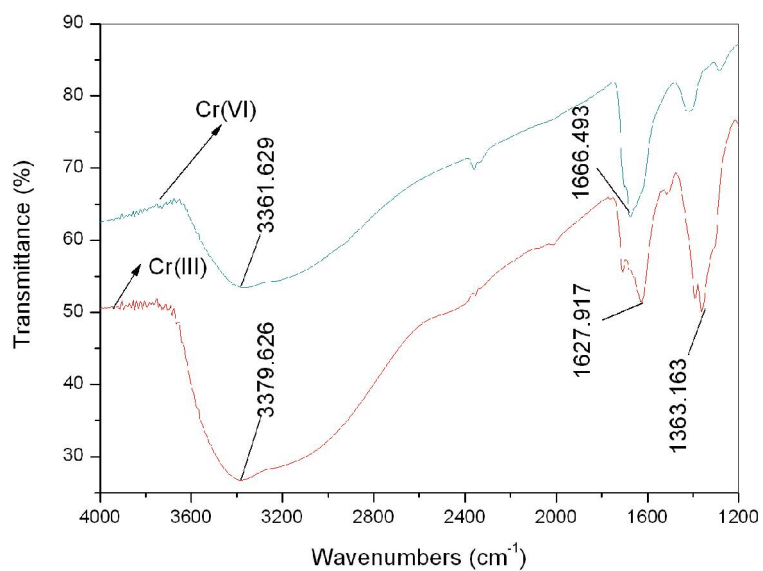


Figure S2. FTIR spectra after 40 min of UV irradiation. Fe(III), 100 μM ; oxalic acid, 500 μM ; Cr(VI) or Cr(III), 640 μM ; pH 3.0. (1363 cm^{-1} , NO_3^- ; 1628-1666 cm^{-1} , C=O stretching vibration of oxalic acid; 3361-3379 cm^{-1} , OH stretching and bending vibration of oxalic acid or water.)

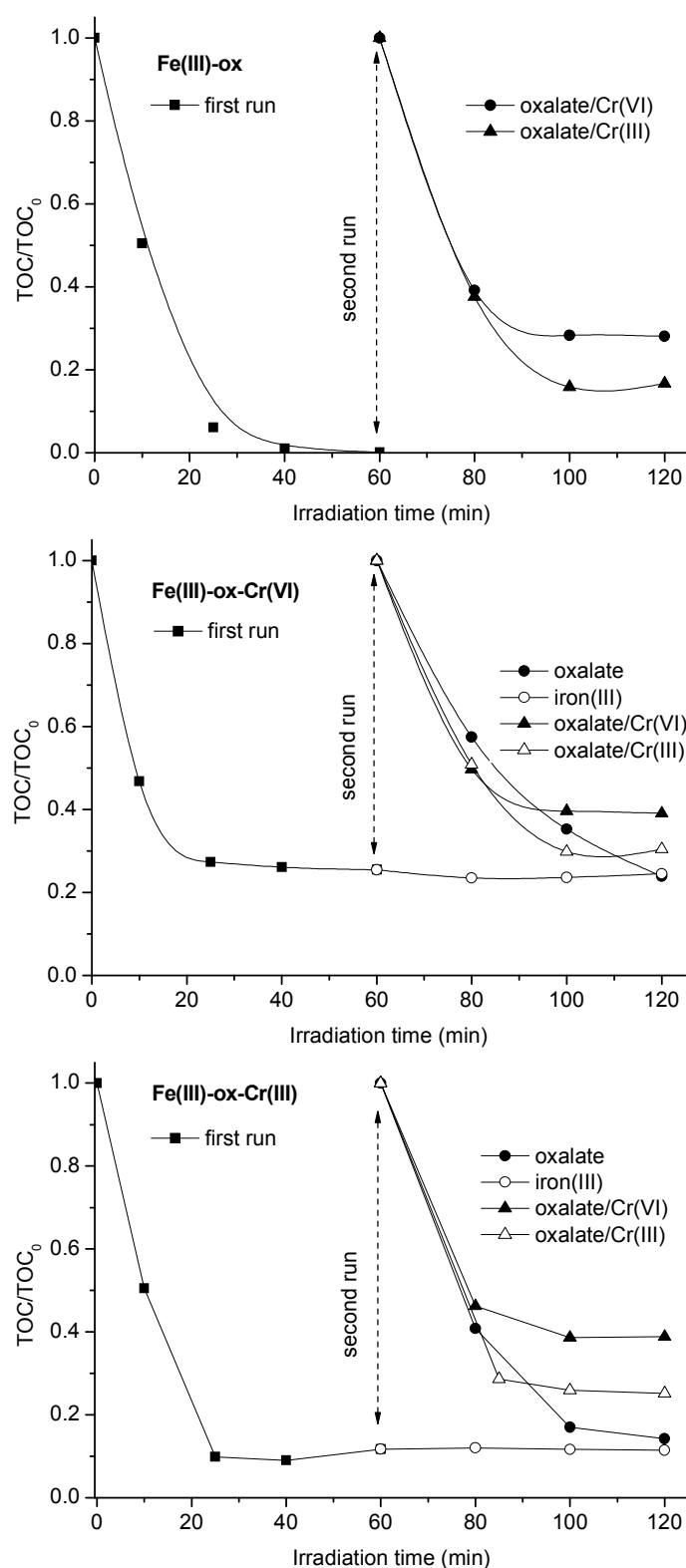


Figure S3. Time profile of Mineralization of oxalate during UV irradiation in the presence or absence of Cr(VI) or Cr(III). For both 1st and 2nd run, if present, Fe(III), 100 μ M; Cr(VI) or Cr(III), 80 μ M; oxalic acid, 500 μ M ; pH 3.0.

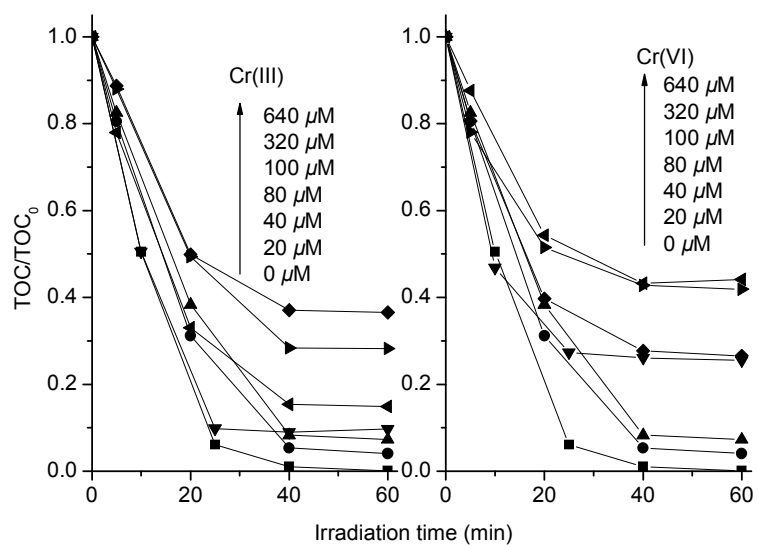


Figure S4. Mineralization of oxalate during UV irradiation in the presence of Cr(VI) or Cr(III). Fe(III), 100 μM; oxalic acid, 500 μM; Cr(VI) or Cr(III), 0-640 μM; pH 3.0.

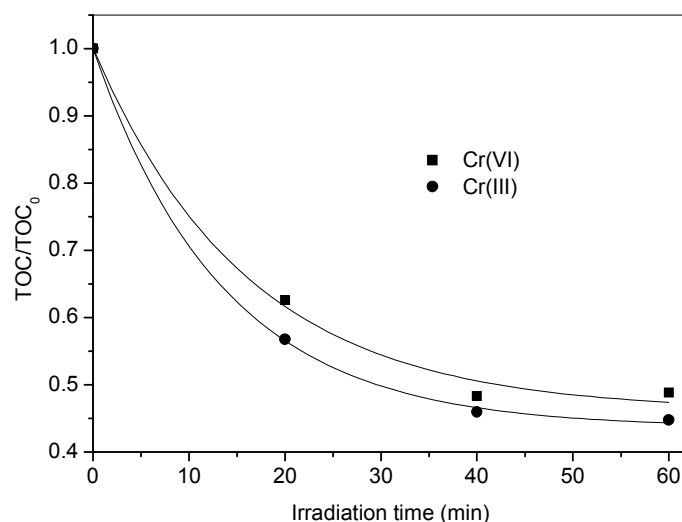


Figure S5. Mineralization of oxalate during UV irradiation in the presence of Cr(VI) or Cr(III). oxalic acid, 200 μM ; pH 3.0. For Cr(VI) system: Fe(III), 76 μM ; Fe(II), 24 μM ; Cr(VI), 512 μM ; Cr(III), 128 μM . For Cr(III) system: Fe(III), 68 μM ; Fe(II), 32 μM ; Cr(VI), 8 μM ; Cr(III), 632 μM .

The selected concentrations of Fe(II)/Fe(III), Cr(VI)/Cr(III) and oxalic acid were on the basis of the results (total Cr 640 μM) in Figure 3 of MS. These concentrations of Fe(II), Cr(VI) and oxalic acid can be experimentally measured whereas the concentration of Fe(III) was obtained by the difference between concentrations of initial Fe and measured Fe(II). Similarly, the Cr(III) concentration was calculated based on the assumption that Cr species only existed as Cr(VI) or Cr(III) state when TOC steady state approached. It is expected that oxalate would have not been degraded if our assumption were correct. The fact that oxalate continued to be degraded suggests that neither Cr(VI) nor Cr(III) but other Cr species are responsible for protecting oxalate from further oxidation.

Two samples for XPS analysis were prepared as follows: after a 50-mL solution containing 100 μM Fe(III), 320 μM Cr(VI) and 500 μM oxalic acid was irradiated for 60 min, the solution was collected and dried under reduced pressure at 30 °C. The obtained solid was redissolved by 0.2 mL water (B) or 0.5 mL acetone (A). The mixture was carefully dropped on the clean silicon chip and then vaporized at room temperature. X-ray photoelectron spectroscopic (XPS) measurement of the samples was carried out on the 2201-XL multifunctional spectrometer (VG Scientific England) using Al K α radiation.

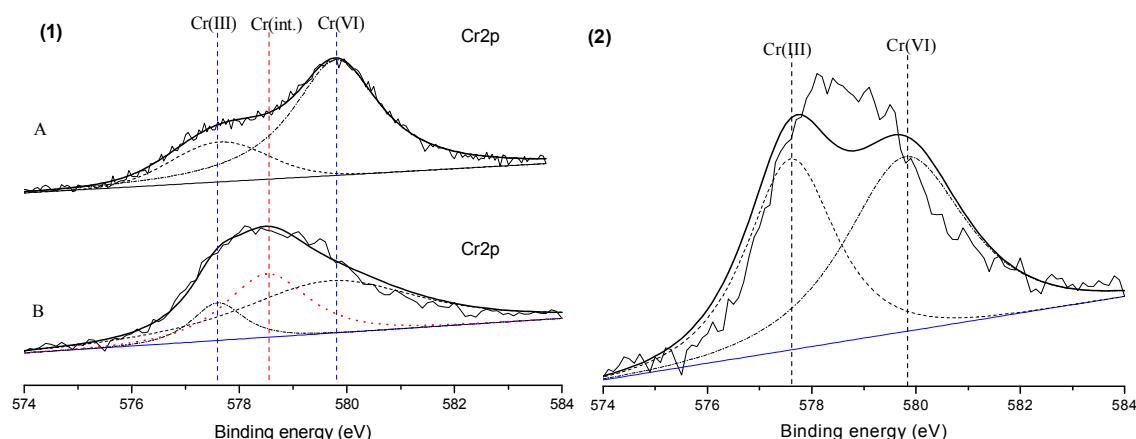


Figure S6. (1) Cr 2p XPS spectra of two samples by different solvent treatment, A-acetone, B-water. For the sample redissolved by acetone (A), the Cr 2p XPS spectra can be perfectly fitted by two peaks located at 577.6 and 579.8 eV, which corresponds to Cr(III) and Cr(VI) respectively. However, For the sample redissolved by water, as shown in Figure S6(2), we failed to fit the spectra well by two peaks at 577.6 and 579.8 eV (1), respectively. But the good curve fitting was achieved by an additional peak at 578.6 eV in Figure S6-1B, which is assigned to Cr intermediates (denoted as Cr(int.)) although their assignments are rarely reported in XPS analysis (1,2). Based on the discussion in MS, we confirm that the intermediate state of Cr exists in the final irradiated solution besides Cr(III) and Cr(VI), which is stable in aqueous solution, but labile to acetone solvent to disproportionate to Cr(III) and Cr(VI). Hence, with choosing acetone as solvent, we could not observe the peak at 578.6 eV in Figure S6-1A.

(1) Daulton, T. L.; Little, B. J. Determination of chromium valence over the range Cr(0)–Cr(VI) by electron energy loss spectroscopy. *Ultramicroscopy* **2006**, *106*, 561-573.

(2) Banerjee, D.; Nesbitt, H. W. Oxidation of aqueous Cr(III) at birnessite surfaces: constraints on reaction mechanism. *Geochimica et Cosmochimica Acta* **1999**, *63*, 1671-1687

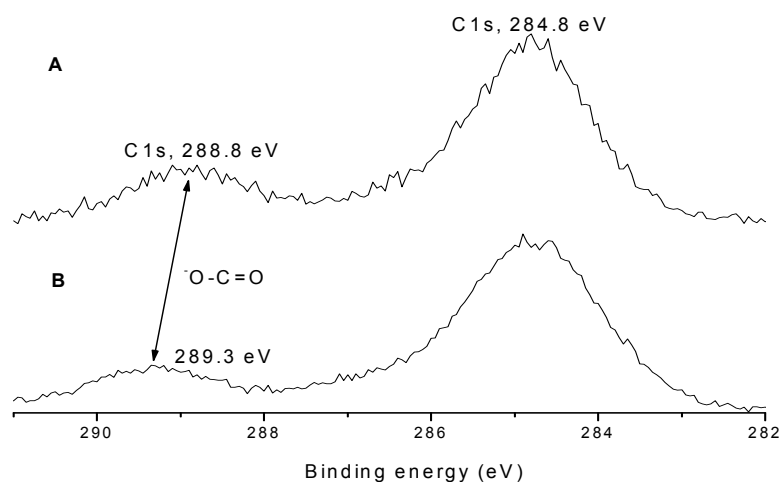


Figure S7. C 1s XPS spectra of two samples by different solvent treatment, (A)-acetone, (B)-water. The peak at 288.8-289.3 eV is ascribed to C 1s of carboxyl (COO^-). The slight shift of the peak location between A and B indicates the difference of coordination environment of carboxyl: the former is probably free of complexation due to the destruction by acetone; the latter one shifts towards high binding energy because of its strong coordination with Cr species. These C 1s spectra may provide further evidence for the terminal state of organic carbon, namely, which exists as oxalate only.

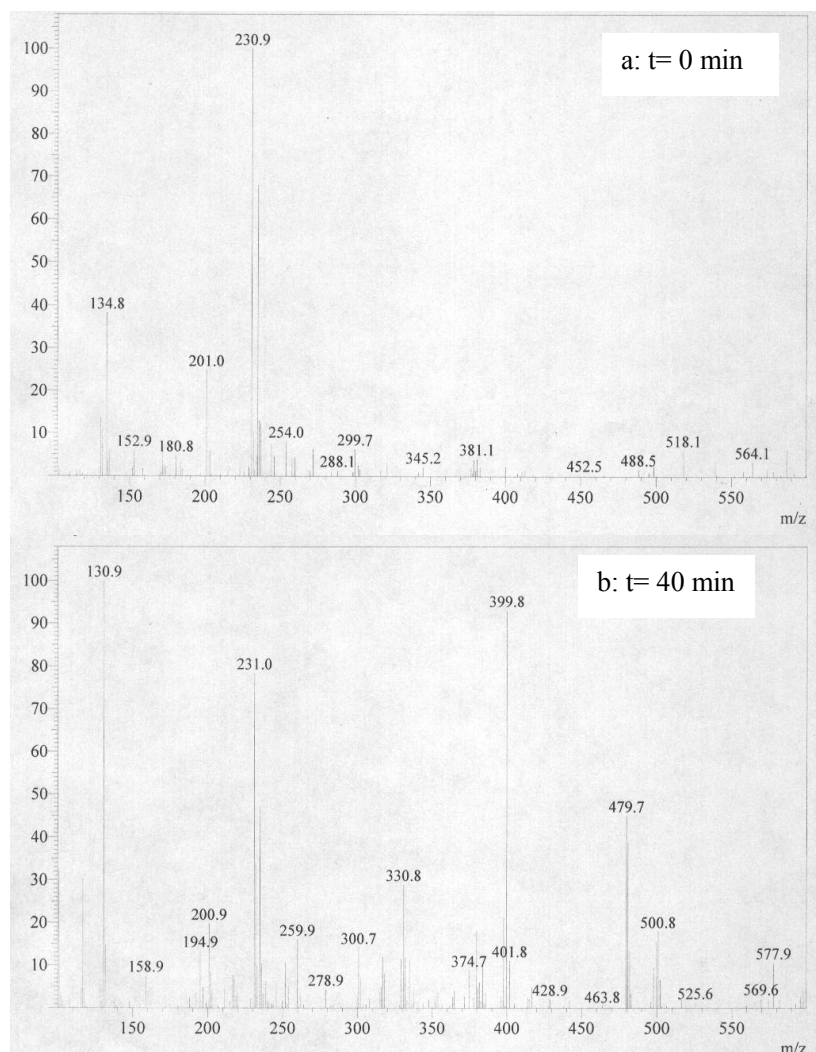
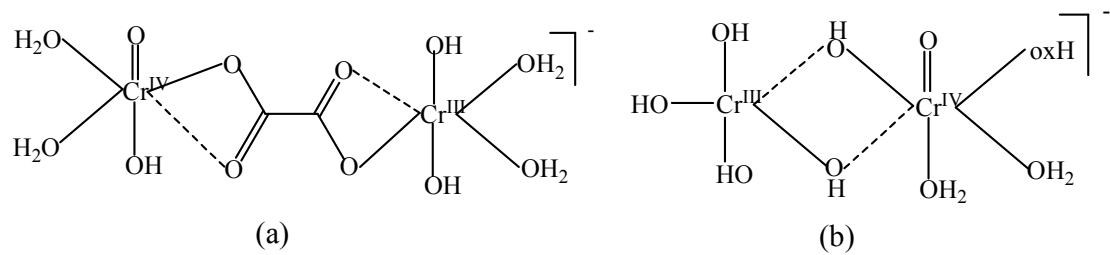


Figure S8. ESI mass spectral patterns (negative ionization mode) (a) before and (b) under UV irradiation for 40 min. Fe(III), 100 μ M; oxalic acid, 500 μ M; Cr(VI), 640 μ M; pH 3.0.

Table S1. Main identified products in ESI-MS spectra.

No.	m / z	formula
1	330.8	$[\text{Cr}_2\text{C}_2\text{O}_{12}\text{H}_{11}]^-$
2	379.8	$[\text{Cr}_3\text{C}_2\text{O}_{12}\text{H}_8]^-$
3	399.8	$[\text{Cr}_2\text{C}_4\text{O}_{15}\text{H}_8]^-$
4	479.7	$[\text{Cr}_3\text{C}_2\text{O}_8\text{H}_{12}]^-$
5	499.8	$[\text{Cr}_3\text{C}_4\text{O}_{18}\text{H}_8]^-$

The new emerging peaks in ESI-MS (b) are assigned to Cr-oxalate complexes in terms of following reasons: 1) iron is excluded in these complexes, owing to the fact that iron can lead to further oxalate degradation in the photochemical process when additional oxalate was added into the solution where the TOC steady state has approached (see Figure S3). It means that iron freely exist in solution rather than being trapped in some complexes; 2) oxalate is resistant to full degradation, as discussed in MS, should be in the form of Cr-ox instead of Fe-ox.



Scheme S1. Proposed oxalate-bridged (a) and oxo-bridged (b) dinuclear Cr-oxalate complexes ($m/z = 330.8$)

Table S2. Selected global chromium concentrations in waters, sediments and surface soils

Date	location	type of environment	Cr(VI)	Cr(total)	reference
2002	Hanford, USA	leakage from HLW ^a fluids	—	50.9-413 mmol L ⁻¹	Qafoku et al. ¹
1998-2000	South Lanarkshire, U.K.	surface water	>90% in total Cr	0.11-6.7 mg L ⁻¹	Farmer et al. ²
		ground water		≤ 91 mg L ⁻¹	
2003	Porto-Romano, Albania	lagoonal and pond sediments	~2,230 mg kg ^{-1 b}	1,130-24,409 mg kg ⁻¹	Shtiza et al. ³
1998-1999	Slag heap in northern France	ground water	0.26-210 mg L ⁻¹		Loyaux-Lawniczak et al. ⁴
1996	Bay of Bengal, India	coastal sediments	—	118 µg g ⁻¹	Selvaraj et al. ⁵
1994	Minatitlan, Mexico	sediments from coatzacalcos river	—	19.25-152.69 mg kg ⁻¹	Rosales-Hoz and Carranza-Edwards ⁶
1959	Upper Mystic Lake, USA	sediments at 35 cm	—	8000-8500 mg kg ⁻¹	Spliethoff and Hemond ⁷
1995	Italy	tannery wastes	spent bath: Cr(III), 3500-4000 mg L ⁻¹ segregated wastewaters: Cr(III), 100-500 mg L ⁻¹		Petruzzelli et al. ⁸
1997-1998	California, USA	contaminated estuary sediments		4.67-14.7 µmol g ⁻¹ dry wt	O'Day et al. ⁹
2001-2002	California, USA	aromas red sands aquifer	~84% in total Cr	5-39 µg L ⁻¹	Gonzalez et al. ¹⁰
1997	Amsterdam and Rotterdam, Netherlands	coastal sediments	—	61-142 mg kg ⁻¹ dry wt	de Boer et al. ¹¹
2000-2001	western Ross Sea, Italy	seawater, 20-1580 m depth	—	1.3-6.2 nmol kg ⁻¹	Corami et al. ¹²
2001	Aveiro, Portugal	urban parks	—	6.0-15 mg kg ⁻¹	Madrid et al. ¹³
2001	Glasgow, U.K.	Glasgow green park	—	24-34 mg kg ⁻¹	Madrid et al. ¹³
2001	Glasgow, U.K.	Alexandra park	—	21-131 mg kg ⁻¹	Madrid et al. ¹³
2001	Ljubljana, Slovenia	urban parks	—	13-33 mg kg ⁻¹	Madrid et al. ¹³
2001	Sevilla, Spain	urban parks	—	21-51 mg kg ⁻¹	Madrid et al. ¹³
2001	Torino, Italy	urban parks	—	150-288 mg kg ⁻¹	Madrid et al. ¹³
2001	Uppsala, Sweden	urban parks	—	7.0-34 mg kg ⁻¹	Madrid et al. ¹³
1999	petroleum refinery area, Jordan	street dust	—	6-160 µg g ⁻¹	Momani et al. ¹⁴
2005	Qinghai, China	contaminated soils around chromium slag dump	—	69.2-179.8 mg kg ⁻¹	Luo and Qu ¹⁵
Last two centuries	Mont Blanc in the French-Italian Alps	snow and ice	—	8 to 469 pg g ⁻¹	Van de Velde et al. ¹⁶
1989	Humber, U.K.	estuary	—	0.17-6.17 µg L ⁻¹	Hunt and Hedgecott ¹⁷
1993	Humber, U.K.	estuary	0.0-0.88 µg L ⁻¹	0.17-2.1 µg L ⁻¹	Gardner and Ravenscroft ¹⁸

^a HLW, high-level radioactive waste.^b Cr(VI) leached from a sample containing a total concentration of Cr 12,200 mg kg⁻¹.

1. Qafoku, N. P.; Ainsworth, C. C.; Szecsody, J. E. *Reactive Transport of Al-rich, Alkaling and Saline High Level Waste Simulants in the Hanford Sediments*; Pacific Northwest Laboratory: Richland, WA, 2002.
2. Farmer, J. G.; Thomas, R. P.; Graham, M. C.; Geelhoed, J. S.; Lumsdon, D. G. Paterson, E. Chromium speciation and fractionation in ground and surface waters in

- the vicinity of chromite ore processing residue disposal sites. *J. Environ. Monit.* **2002**, *4*, 235–243.
3. Shtiza, A.; Swennen, R.; Tashko, A. Chromium speciation and existing natural attenuation conditions in lagoonal and pond sediments in the former chemical plant of Porto-Romano (Albania). *Environ. Geol.* **2008**, *53*, 1107–1128.
 4. Loyaux-Lawniczak, S.; Lecomte, P.; Ehrhardt, J.-J. Behavior of hexavalent chromium in a polluted groundwater: redox processes and immobilization in soils. *Environ. Sci. Technol.* **2001**, *35*, 1350–1357.
 5. Selvaraj, K.; Mohan, V. R.; Szefer, P. Evaluation of metal contamination in coastal sediments of the Bay of Bengal, India: geochemical and statistical approaches. *Mar. Pollut. Bull.* **2004**, *49*, 174–185.
 6. Rosales-Hoz, L.; Carranza-Edwards, A. Heavy Metals in Sediments from Coatzacoalcas River, Mexico. *Bull. Environ. Contam. Toxicol.* **1998**, *60*, 553–561.
 7. Spliethoff, H. M.; Hemond, H. F. History of toxic metal discharge to surface waters of the Aberjona watershed. *Environ. Sci. Technol.* **1996**, *30*, 121–128.
 8. Petruzzelli, D.; Passino, R.; Tiravanti, G. Ion exchange process for chromium removal and recovery from tannery wastes. *Ind. Eng. Chem. Res.* **1996**, *34*, 2612–2617.
 9. O'Day, P. A.; Carroll, S. A.; Randall, S.; Martinelli, R. E.; Anderson, S. L.; Jelinski, J.; Knezovich, J. P. Metal speciation and bioavailability in contaminated estuary sediments, alameda naval air station, California. *Environ. Sci. Technol.* **2000**, *34*, 3665–3673.
 10. Gonzalez, A. R.; Ndung'u, K.; Flegal, A. R. Natural occurrence of hexavalent chromium in the aromas red sands aquifer, California. *Environ. Sci. Technol.* **2005**, *39*, 5505–5511.
 11. de Boer, J.; van der Zande, T. E.; Pieters, H.; Ariese, F.; Schipper, C. A.; van Brummelen, T.; Vethaak, A. D. Organic contaminants and trace metals in flounder liver and sediment from the Amsterdam and Rotterdam harbours and off the Dutch coast. *J. Environ. Monitor.* **2001**, *4*, 386–393.
 12. Corami, F.; Capodaglio, G.; Turetta, C.; Soggia, F.; Magi, E.; Grotti, M. Summer distribution of trace metals in the western sector of the Ross Sea, Antarctica. *J. Environ. Monit.* **2005**, *12*, 1256–1264.
 13. Madrid, L.; Diaz-Barrientos, E.; Ruiz-Cortés, E.; Reinoso, R.; Biasioli, M.; Davidson, C. M.; Duarte, A. C.; Grčman, H.; Hossack, I.; Hursthouse, A. S.; Kralj T.; Ljung, K.; Otabbong, E.; Rodrigues, S.; Urquhart, G. J.; Ajmone-Marsan, F. Variability in concentrations of potentially toxic elements in urban parks from six European cities. *J. Environ. Monit.* **2006**, *11*, 1158–1165.
 14. Momani, K. A.; Jaradat, Q. M.; Jbarah, A. E.-A. Q.; Omari, A. A.; Al-Momani, I. F. Water-soluble species and heavy metal contamination of the petroleum refinery area. Jordan. *J. Environ. Monitor.* **2002**, *6*, 990–996.
 15. Luo, J. F.; Qu, D. Study on the Soil Cr Pollution in Residue Piling Yard in Qinghai Province. *Acta Agriculturae Boreali-occidentalis Sinica (in Chinese)* **2006**, *15*, 244–247.
 16. Van De Velde, K.; Ferrari, C.; Barbante, C.; Moret, I.; Bellomi, T.; Hong, S. M.; Boutron, C. A 200 year record of atmospheric cobalt, chromium, molybdenum, and antimony in high altitude alpine firn and ice. *Environ. Sci. Technol.* **1999**, *33*, 3495–3501.
 17. Hunt, D. T. E.; Hedgecott, S. *Revised Environmental Quality Standards for Chromium in Water*, Final Report to the Department of the Environment, 1994.
 18. Gardner, M. J.; Ravenscroft, J. E. Determination of chromium(III) and total chromium in marine waters. *Fresenius' J. Anal. Chem.*, **1996**, *354*, 602–605.

Discussion on Inner filter effect

Inner filter effect should be considered when several components absorb light at the excitation wavelength or photoproduct species itself absorb a fraction of light. (Lees, A. J. *Anal. Chem.* **1996**, 68, 226–229; Lees, A. J. *Coord. Chem. Rev.* **2001**, 211, 255–278).

During our irradiation experiments, 100 W Hg lamp (Toshiba SHL-100UVQ-2) is chosen for light source, which mainly emits at 365 nm within UVA region (320–400 nm). Figure R1 shows the UV-vis absorption spectra for the solutions containing Fe(III)-ox-Cr(III) (a) and Fe(III)-ox-Cr(VI) (b). Cr(III)-ox species (**line 2**) does not absorb light within the range of 300–400 nm, thus not contributing to the total absorbance in the UVA region. For Cr(VI)-ox complexes (**line 5**), there are two major absorption peaks at 256 nm (ϵ_{256} , $1625 \text{ M}^{-1} \text{ cm}^{-1}$) and 350 nm (ϵ_{350} , $2487.5 \text{ M}^{-1} \text{ cm}^{-1}$), respectively. However, the quantum efficiency for Cr(III)-ox or Cr(VI)-ox is very low because of TOC change by <10% during 60 min of irradiation, whereas oxalate in Fe(III)-ox alone has been depleted completely during the same period (see Figure 2 in MS).

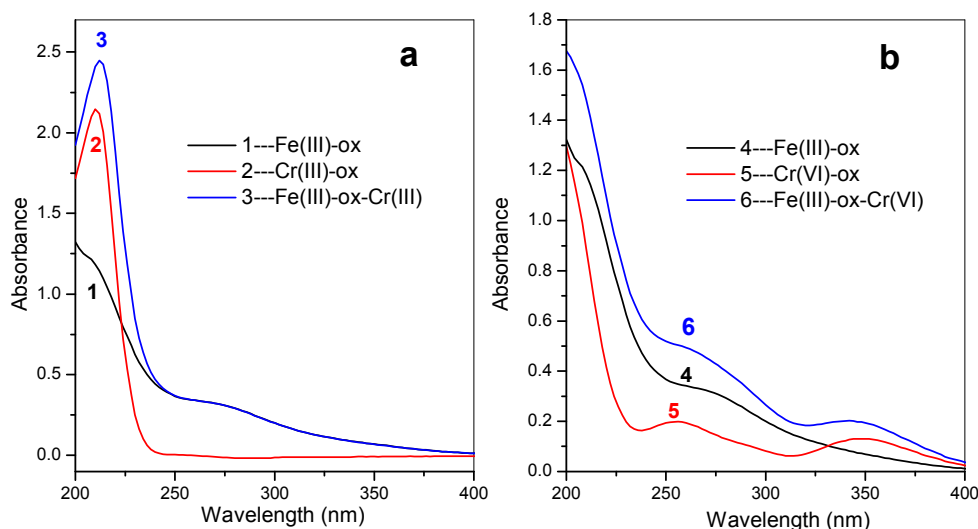


Figure S9. UV-vis absorption spectra changes of Fe(III)-ox-Cr(III) (a) and Fe(III)-ox-Cr(VI) (b) solutions accompanying continuous UV irradiation. Fe(III), 100 μM ; oxalic acid, 500 μM ; Cr(III)/Cr(VI), 80 μM ; pH 3.0.

Within wide spectral range (200–400 nm), Cr(VI) species absorption overlaps considerably that of the Fe(III)-ox complexes (**line 1 or 4**) (including Fe(ox)^+ , Fe(ox)_2^- , Fe(ox)_3^{3-} , Zuo, Y. G; Holgné, J. *Environ. Sci. Technol.* **1992**, 26, 1014–1022.; Hug, S. J.; Laubscher, H-U.; James, B. R. *Environ. Sci. Technol.* **1997**, 31, 160–170). At the early stage of photochemical reactions, Cr(VI) components would absorb a fraction of the UVA light and further decrease the quantum efficiency for photolysis of Fe(III)-ox complexes. However, Cr(VI) would be rapidly reduced by Fe(II) and $\text{CO}_2^{\cdot-}$ within 5 min (see Figure 1b in MS, also in Hug's article: Hug, S. J.; Laubscher, H-U.; James, B. R. *Environ. Sci. Technol.* **1997**, 31,

160-170), and does not continue to compete light absorption with iron complexes. Therefore, the *inner filter effect* of Cr(VI) components was not further considered in detail in the current manuscript, although it is interesting for further research. Figure R2 shows the UV-vis absorption spectra of two systems (i.e. Fe(III)-ox-Cr(VI) and Fe(III)-ox-Cr(III)) after 60 min of UV irradiation. These spectra suggest that the photoreaction products of two systems can not absorb light within the spectral range of 300-400 nm. It means that Fe(III)-ox species are still supposed to be the dominant components that absorb UV light throughout the photolysis experiments before the oxalate is consumed completely.

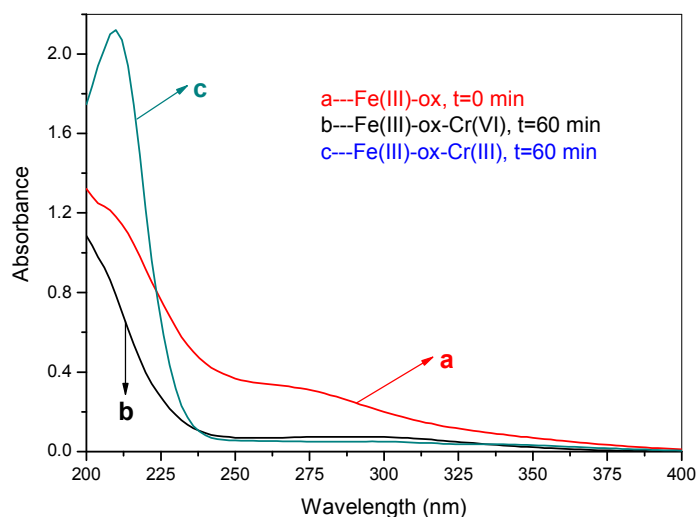


Figure S10. UV-vis absorption spectra of initial Fe(III)-ox (a), Fe(III)-ox-Cr(VI), t=60 min (b) and Fe(III)-ox-Cr(III), t=60 min (c) solutions. Fe(III), 100 μ M; oxalic acid, 500 μ M; Cr(III)/Cr(VI), 80 μ M; pH 3.0.